Spray Coatable Electrochromic Dioxythiophene Polymers with High Coloration Efficiencies

Benjamin D. Reeves,[†] Christophe R. G. Grenier,[†] Avni A. Argun,[†] Ali Cirpan,[†] Tracy D. McCarley,[‡] and John R. Reynolds*[,†]

Department of Chemistry, Center for Macromolecular Science and Engineering: University of Florida, Gainesville, Florida 32611-7200, and Department of Chemistry, Louisiana State University, Baton Rouge, Louisiana 70803-1804

Received April 21, 2004; Revised Manuscript Received July 14, 2004

ABSTRACT: Four new disubstituted propylenedioxythiophene polymers have been synthesized by Grignard metathesis on the 1−5 g scale. All polymers were found to be soluble in chloroform, methylene chloride, toluene, and tetrahydrofuran and were fully structurally characterized having GPC determined number-average molecular weights ranging from 33000 to 47000 g mol^{-1}. Dilute polymer solutions in toluene exhibited strong red fluorescence with moderate quantum efficiencies from 0.38 to 0.50. Homogeneous thin films were formed by electropolymerization and spray casting polymer solutions onto ITO coated glass slides at thicknesses of ca. 150 nm. The films were electroactive, switching from a dark blue-purple to a transmissive sky blue upon p-doping, often with subsecond switching times, and high electrochromic contrast luminance changes (% ΔY) of 40−70%. These studies revealed that the branched derivatives, [poly(3,3-bis(2-ethylhexyl)-3,4-dihydro-2*H*-thieno[3,4-*b*][1,4]dioxepine)] and [poly(6,8-dibromo-3,3-bis(2-ethylhexyloxymethyl)-3,4-dihydro-2*H*-thieno[3,4-*b*][1,4]dioxepine)], gave an electrochemical response and associated color change over a much smaller voltage range in comparison to the linear chain substituted derivatives, [poly(3,3-dihexyl-3,4-dihydro-2*H*-thieno[3,4-*b*][1,4]dioxepine)] and [poly(3,3-bis-(octadecyloxymethyl)-3,4-dihydro-2*H*-thieno[3,4-*b*][1,4]dioxepine)]. Composite coloration efficiency values were found up to 1365 cm^2/C; this was considerably larger than values obtained from previously studied alkylenedioxythiophene based polymers (∼375 cm^2/C).

Introduction

Great effort has been made over the last 2 decades to study and utilize the electronic properties of thiophene-based conducting polymers while optimizing their processability.[1−3] This has led to the use of polythiophenes in various applications including light emitting devices,[4] chemical sensors,[5] rechargeable batteries,[6] organic thin film transistors,[7] and electrochromic devices.[8] Processability of polythiophenes has undergone vast improvements by derivatizing the 3-position of the ring with flexible substituents.[9−11] The regioregularity of these poly(3-alkyl thiophenes) (p3AT's) plays an important role in property control.[12] Models of regiorandom, regioregular, and regiosymmetric polymers are illustrated in Scheme 1. If the unsymmetrical monomer only couples in a head-to-tail fashion, the alkyl substituents do not interfere with the conjugation of the thiophene rings via steric interactions, and the resulting polymer is regioregular.

While numerous methods[12,13] have been employed for synthesizing regioregular p3AT's, the latest method developed by McCullough and co-workers, Grignard metathesis polymerization, does not require long reaction times, cryogenic temperatures, or nontrivial preparation of reagents often seen with other methods.[14,15]

Poly(thiophenes) show excellent potential for use in electrochromic devices due to the drastic change in the electromagnetic spectrum upon charge injection (doping) with the parent polymer switching from red to blue upon oxidation.[16] Derivitizing the 3- and 4-positions of the thiophene ring with an alkylenedioxy brigde lowers the band gap and the oxidation potential due to the two electron donating oxygen atoms.[17,18] Poly(3,4-ethylenedioxythiophene) (PEDOT) is cathodically coloring, switching between a dark blue in the neutral state and a transmissive sky blue in the oxidized state.

Scheme 1

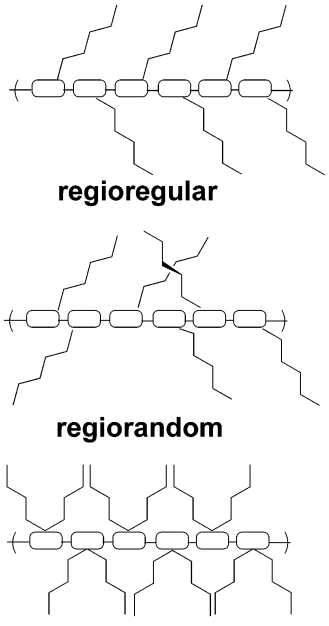

By taking advantage of the synthetic flexibility of the PEDOT monomer structure, we have been successful in synthesizing and studying the electrochromic properties of many derivatives of PEDOT.[19−22] We have developed synthetic methodologies to vary the alkylene-

* Corresponding author. E-mail: reynolds@chem.ufl.edu.
[†] University of Florida.
[‡] Louisiana State University.

10.1021/ma049222y CCC: $27.50
Published on Web 09/04/2004

Scheme 2

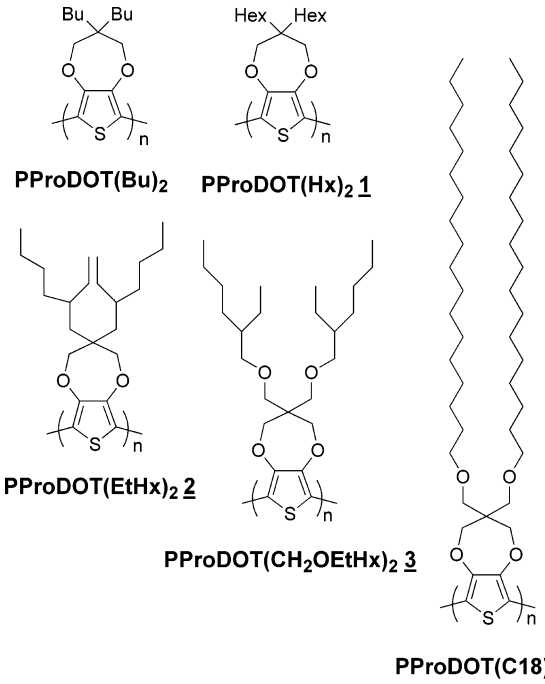

dioxy ring size, and vary the size, number, and placement of substituents on the ring by utilizing Williamson etherfication,[20] transetherification,[21,22] and Mitsunobu chemistry.[23] A dimethyl derivative of propylenedioxythiophene, PProDOT(Me)$_2$, exhibits a contrast ratio of 78% at 585 nm and a switching time of 0.3 s, the best values obtained from the alkylenedioxythiophene family.[21] With small substituents, electropolymerization is used for film formation.[24]

In developing disubstituted poly(3,4-propylenedioxythiophenes), we utilized the C_2 symmetry of the propylenedioxythiophene monomer to form a regiosymmetric polymer and induce solubility in organic solvents.[25] As the propylenedioxy ring functions as a spacer to separate the alkyl chains from the polymer backbone, there is a minimal effect on the extent of conjugation. Grignard metathesis coupling was utilized in the synthesis of a soluble and processable dibutyl derivative of poly(3,4-propylenedioxythiophene), **PProDOT(Bu)$_2$** (Scheme 2).

In this work, the synthesis of four new poly(alkylenedioxythiophenes) by Grignard metathesis is reported. Scheme 2 depicts the four polymer structures, **1**−**4**. All of these polymers, as with **PProDOT(Bu)$_2$**, were synthesized from regiosymmetric monomers to yield regiosymmetric polymers and are soluble in organic solvents, allowing facile characterization of the molecular weight by GPC and primary structure by ^{13}C and ^{1}H NMR. This solubility also allowed polymer solutions to be spray cast onto working electrodes and the electrochemical and electrochromic properties of the films to be analyzed. The electrochemical polymerization of each monomer was also performed and the electrochromism of spray cast and electrochemically deposited films were compared. Finally, coloration efficiency studies show these polymers to behave as efficient, high contrast electrochromic materials, useful for electrochromic devices.[26]

Results and Discussion

Monomer Synthesis. The synthesis of alkoxy-derivitized ProDOT monomers was accomplished by first carrying out a transetherification of 3,4-dimethoxythiophene with 2,2-bis(bromomethyl)-1,3-propanediol to form **ProDOT(CH$_2$Br)$_2$**, as shown in Scheme 3.

Scheme 3

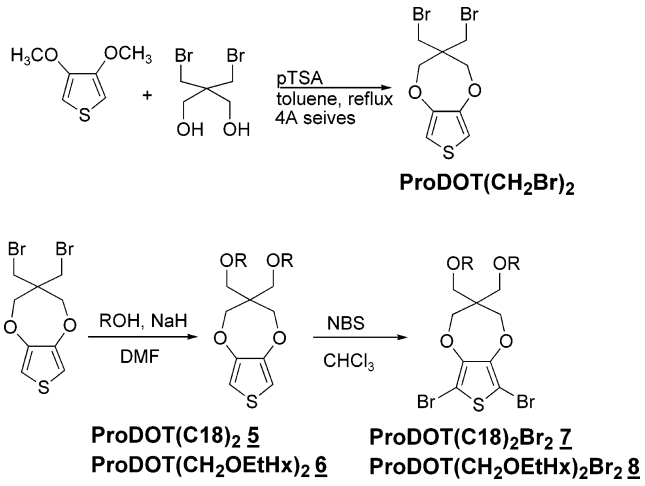

Scheme 4

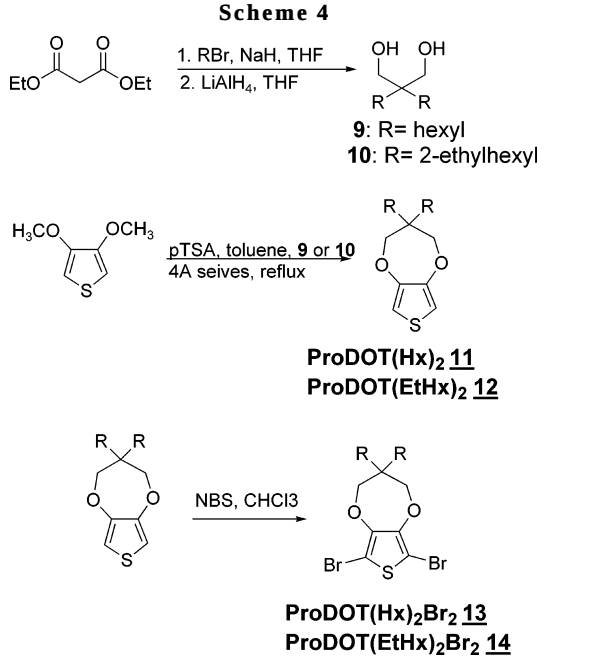

ProDOT(CH$_2$Br)$_2$ can be used as a precursor to form any number of structures which can be synthesized by a Williamson etherification to afford the electrochemically polymerizable monomers, **ProDOT(C18)$_2$** (**5**) and **ProDOT(CH$_2$OEtHx)$_2$** (**6**). Figure 1a shows the ^{1}H NMR of **ProDOT(C18)$_2$** (**5**). The singlet at 6.44 ppm corresponds to the thienyl protons while the singlets at 4 and 3.48 correspond to the methylene protons of the propylenedioxy bridge and the methoxy ether substituent groups, respectively. The octadecyl groups give rise to the signals at 3.36 (triplet, O−C**H$_2$**C$_{17}$H$_{35}$), 0.88 (triplet, C**H$_3$**C$_{17}$H$_{35}$O−), and 1.5 (multiplet, O−CH$_2$C$_{16}$**H$_{32}$**CH$_3$) ppm.

Next, the thiophene ring was brominated at the 2- and 5-positions using NBS. The ^{1}H NMR of **ProDOT(C18)$_2$Br$_2$** (**7**) given in Figure 1b differs from **ProDOT(C18)$_2$** (**5**) by only the absence of the thienyl proton signal at 6.4 ppm, as expected.

As seen in Scheme 4, alkyl substituents can also be placed on the 2-position of the propylenedioxy ring by first synthesizing the desired diol by an alkylation of diethyl malonate using sodium hydride and the corre-

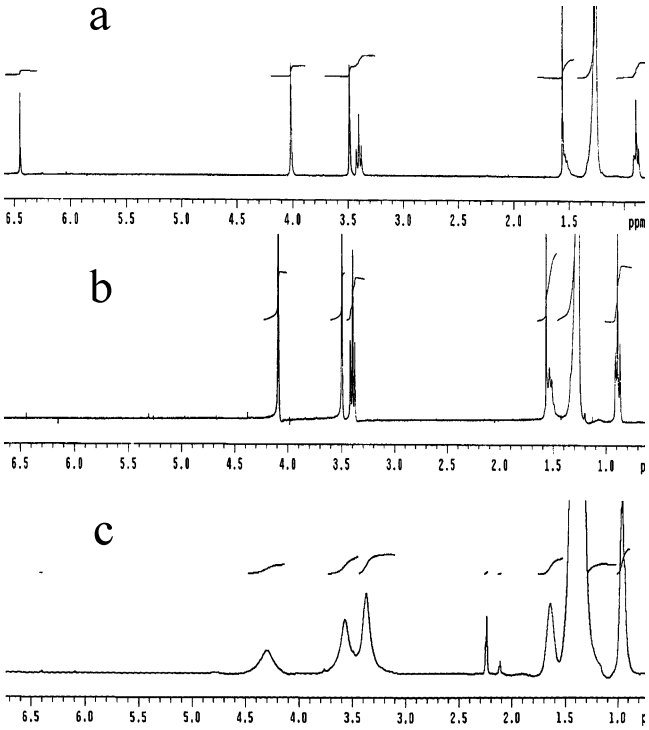

Figure 1. ^{1}H NMR of (a) **ProDOT(C18)$_2$** (**5**), (b) **ProDOT-(C18)$_2$Br$_2$** (**7**), and (c) **PProDOT(C18)$_2$** (**4**), after end group conversion to hydrogens by subjecting to *n*BuLi followed by an aqueous work up.

sponding alkyl bromide followed by an $LiAlH_4$ reduction.[27] The diol, **9**, was synthesized on a 300 g scale in good yield.

Electrochemically polymerizable monomers, **ProDOT-(Hx)$_2$** (**11**) and **ProDOT(EtHx)$_2$** (**12**), were formed by a transetherification reaction of 3,4-dimethoxythiophene with the corresponding diol. The chemically polymerizable monomers, **ProDOT(Hx)$_2$Br$_2$** (**13**) and **ProDOT-(EtHx)$_2$Br$_2$** (**14**), were obtained by bromination of **ProDOT(Hx)$_2$** (**11**) and **ProDOT(EtHx)$_2$** (**12**) using NBS followed by column chromatography. The methodology used in Scheme 4 has generated the monomer, **ProDOT(Hx)$_2$Br$_2$** (**13**), on a 10 g scale.

Polymer Synthesis. As seen in Scheme 5, all monomers underwent Grignard metathesis polymerization. First, a titrated methylmagnesium bromide solution was added slowly to the monomer in dry THF and the solution was refluxed for 1 h. Ni(dppp)Cl_2 was added immediately turning the solution from clear pink to bright red. The mixture was heated at reflux for 20 h followed by precipitation of the polymer into methanol. The solid was filtered into a cellulose thimble and placed in a Soxhlet apparatus for fractionation. Methanol was refluxed over the thimble for 24 h to remove the monomer and salts, followed by hexanes for 48 h to remove oligomers. Finally, methylene chloride or chloroform was refluxed over the thimble to remove the pure polymer. After removing the solvent by rotary evaporation, a dark purple solid was obtained, which was soluble in $CHCl_3$, CH_2Cl_2, THF, toluene, and benzene. As the size of the substituent increases, the solubility increases. Polymers **1**−**4** gave solubilities of 13, 36, 57, and 124 mg/mL in toluene, respectively. The polymers were characterized by ^{13}C and ^{1}H NMR and gave results as expected (see Experimental Section). A 10 mg sample of **PProDOT(C18)$_2$** (**4**) was reacted with ^{n}BuLi followed by an aqueous work up to convert the end groups to

Scheme 5

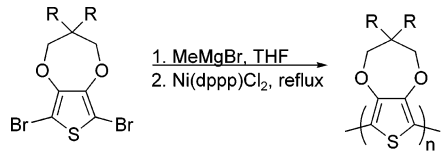

PProDOT(Hx)$_2$ 1
PProDOT(EtHx)$_2$ 2
PProDOT(CH$_2$OEtHx)$_2$ 3
PProDOT(C18)$_2$ 4

Table 1. Molecular Weight Determination by GPC

	M_n(GPC)	M_w	X_n	PDI
1	38100	65900	117	1.73
2	43000	62600	113	1.46
3	47300	74800	107	1.58
4	33400	48000	46	1.43

hydrogens.[28] The ^{1}H NMR spectrum of the sample (Figure 1c) gives broad signals, typical for a polymer, and the thienyl proton end groups are undetectable as expected for a polymer of substantial molecular weight.

Molecular Weight Characterization. Molecular weight analyses of the purified polymers were performed by GPC (see Table 1) and MALDI−TOF MS. The GPC results gave number-average molecular weights ranging from 33000 to 47000 g mol^{-1} and weight-average molecular weights between 47000 and 75000 g mol^{-1} with polydispersity ranging from 1.43 to 1.73 after fractionation during purification. These high molecular weights do not likely affect the optical or electronic properties of these polymers[29] but do enhance film forming ability, leading to easier processing. The high molecular weights obtained are as expected since the polymer solutions spray cast to form homogeneous thin films (discussed later in **Film Preparation**).

The MALDI−TOF MS analyses confirmed the presence of chains of molecular weights of up to 10000 g mol^{-1} for **PProDOT(CH$_2$OEtHx)$_2$** (**3**) and **PProDOT-(C18)$_2$** (**4**) and up to 5000 g mol^{-1} for polymers **PProDOT(Hx)$_2$** (**1**) and **PProDOT(EtHx)$_2$** (**2**). These values are in no way limiting or average due to the inability of longer chains to be volatized. The MALDI spectra of polymers **PProDOT(Hx)$_2$** (**1**), **PProDOT(CH$_2$OEtHx)$_2$** (**3**), and **PProDOT(C18)$_2$** (**4**) exhibited intense ion series that were separated by the expected mass of the repeat unit of the polymer for each case. **PProDOT-(EtHx)$_2$** (**2**) only gave a weak signal that tailed off at *m*/*z* 5000. Further work is underway to improve the ion signal-to-noise ratio. Figure 2 shows the spectrum of **PProDOT(CH$_2$OEtHx)$_2$** (**3**). The dominant peaks are separated by 438 amu, corresponding to the mass of the monomer repeat unit, and the residual mass corresponds to two chlorine end groups [(438)*n* + 71 amu]. This is unexpected and differs from earlier studies of polythiophene and poly(alkylenedioxythiophene) synthesized by Grignard metathesis.[25,28] The only chlorine source available must come from the catalyst, Ni(dppp)-Cl_2. Further studies are underway to determine whether the chlorine from the catalyst is terminating polymerization.

Fluorescence Spectroscopy. Polythiophenes are known to exhibit fluorescence in solution and in the solid state and, thus, can be used as components in light emitting diodes[4] and chemical sensors.[5] In earlier work, a photoluminecence study of **PProDOT(Bu)$_2$** discov-

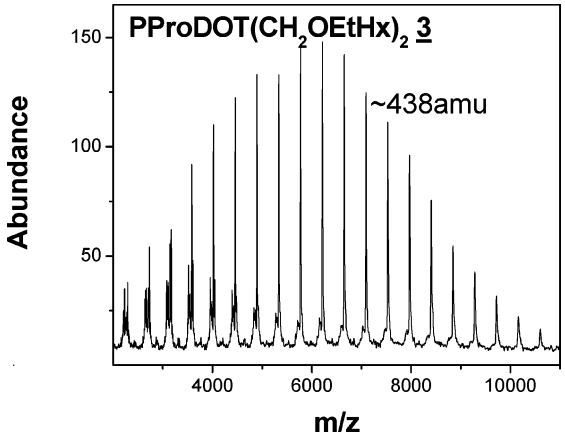

Figure 2. MALDI−TOF of **PProDOT(CH$_2$OEtHx)$_2$ (3)** with HABA matrix. The dominant peaks are roughly 438 amu apart, corresponding to the mass of the monomer repeat unit.

Table 2. Fluorescence Spectroscopy and Quantum Efficiencies

	$\lambda_{(\text{fluorescence})}$[a]	ϕ_{fl}[b]
PProDOT(Bu)$_2$[25]	617, 671	0.45
1	608, 664	0.50
2	624, 678	0.43
3	604, 636	0.38
4	602, 656	0.40

[a] Peaks (nm) from the fluorescence spectra of polymer solutions in toluene. [b] Fluorescence quantum efficiency in toluene solution.

ered polymer solutions to have quantum efficiencies of 45% and emit a deep red color.[25] Table 2 shows all of the polymers have moderate quantum efficiencies in toluene solution with emission maxima corresponding to a deep red hue. The red fluorescence of the polymer solutions is observable under fluorescent room lighting. The absorbance and fluorescence spectra of **PProDOT-(Hx)$_2$ (1)** are shown in Figure 3. Two well-defined vibronic bands exist in the fluorescence spectrum at 608 and 664 nm and one poorly resolved band is present at 730 nm. The spacing between each band is approximately 1370 cm,$^{-1}$ most likely corresponding to the C−C vibrational modes of the thiophene ring. A very small Stokes shift of 675 cm^{-1} suggests that there is little geometric change between the ground and excited states. The fluorescence quantum efficiencies range from 0.38 to 0.50 with **PProDOT(Hx)$_2$ (1)** giving the highest value. The fluorescence spectra of drop cast and vacuum dried films of **PProDOT(CH$_2$OEtHx)$_2$ (3)** and **PProDOT(C18)$_2$ (4)** showed the quantum efficiency decreases dramatically in comparison to solution, with values ranging from 0.02 to 0.03. This is most likely due to rapid nonradiative decay at interchain trap sites, which was previously attributed to the low quantum efficiencies of **PProDOT(Bu)$_2$** films.[25]

Thermochromic Studies. Thermochromic studies were performed on all polymer solutions in toluene. Thermochromism is a useful tool to probe conformational changes in conjugated polymers, and can aid in the development of materials suitable for sensors.[30] Figure 4 shows a series of spectra of a solution of **PProDOT(C18)$_2$ (4)** at temperatures between −4 and +85 °C. The spectra blue shift for all solutions from 10 to 20 nm as the temperature increases, as expected. Although solutions of all other polymers stay the same perceivable red color as a function of temperature, solutions of **PProDOT(C18)$_2$ (4)** undergo a distinct transition, changing from red to dark purple, when

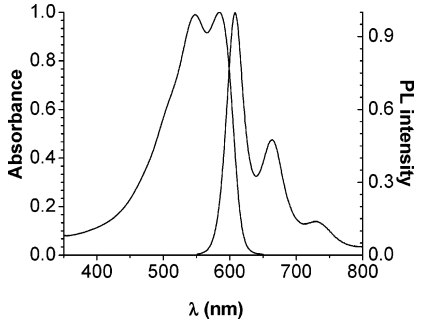

Figure 3. UV−vis absorbance spectrum (left) superimposed upon the fluorescence emission spectrum (right) of a toluene solution of **PProDOT(Hx)$_2$ (1)**.

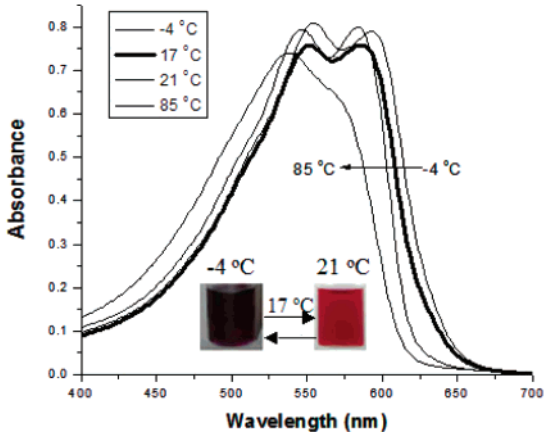

Figure 4. Visible spectra of a polymer solution of **PProDOT-(C18)$_2$** in toluene (1.5 mg/50 mL) taken at −4, +17, +21, and +85 °C. The photographs show the solutions at −4 (left, dark purple) and +21 °C (right, deep red). The colors switch reversibly when crossing +17 °C.

Table 3. Electrochemical Data (V) of PProDOT Derivatives vs Fc/Fc$^+$

	$E_{\text{p,m}}$[a]	$E_{1/2,\text{p}}$[b]	$E_{1/2,\text{p}}$[c]
PProDOT(Bu)$_2$	1.03	−0.19	−0.11
1	1.1	−0.12	0.07
2	1.1	0.05	0.11
3	1.07	0.13	0.20
4	NA[d]	NA[d]	0.11

[a] Monomer oxidation potential. [b] Half-wave potential of the electrochemically polymerized polymer. [c] Half-wave potential of the spray cast polymer from toluene solution. [d] Monomer **ProDOT(C18)$_2$ (5)** could not be electropolymerized.

cooling below 17 °C. Photographs taken at −4 and +21 °C are shown at the bottom of Figure 4.

Film Preparation and Electrochemistry. PProDOT-R$_2$ films were formed by one of two methods. The first method involved the electrochemical deposition onto a working electrode from a 0.01 M monomer/0.1 M tetrabutylammonium hexafluorophosphate (TBAPF$_6$) solution in propylene carbonate. Monomers **ProDOT-(CH$_2$OEtHx)$_2$ (6)**, **ProDOT(Hx)$_2$ (11)**, and **ProDOT-(EtHx)$_2$ (12)** were electrochemically polymerized onto a platinum button or ITO coated glass slide by potenstiostatic deposition using a platinum flag as a counter electrode and a silver wire pseudo reference electrode calibrated using a Fc/Fc$^+$ redox couple. The oxidation potential of the monomers are given in Table 3 and are similar to other alkylenedioxythiophenes at approximately +1 V vs Fc/Fc$^+$. This suggests the long and branched alkyl chain substituents do not effect the oxidation potential of the monomer. **ProDOT(C18)$_2$ (5)**

Table 4. Peaks (λ, nm) and Optical Band Gaps (E, eV) from the UV−vis Spectroscopy of PProDOT Derivatives

	$\lambda_{(echem)}$[a]	$E_{g(echem)}$[b]	$\lambda_{(sol)}$[c]	$\lambda_{(film)}$[d]	$\lambda_{(redox)}$[e]	$E_{g(redox)}$[f]
PProDOT(Bu)$_2$	632, 573, 533	1.86	542	544	576	1.84
1	634, 584	1.80	586, 548	595, 553	575	1.84
2	623, 567, 517	1.96	595, 552	611, 559	618, 543, 521	1.92
3	609, 555, 518	1.87	543	581, 543	600, 551	1.97
4	NA	NA	587, 548	594, 553	590, 559	1.89

[a] Electrochemically polymerized films. [b] Optical band gap of electrodeposited films. [c] 1 mg/mL solution in toluene. [d] Spray cast films from 5 mg/mL polymer solutions in toluene. [e] Spray cast films from toluene solution that were switched from neutral to the oxidized state and back to the neutral state. [f] Optical bangap of a previously switched spray cast film.

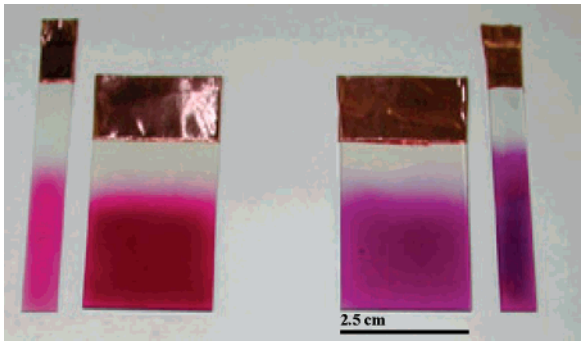

Figure 5. Photograph of spray cast films of PProDOT(CH$_2$-OEtHx)$_2$ (**3**) (red, left) and **PProDOT(C18)$_2$** (**4**) (purple, right) from 5 mg/mL toluene solutions using an air brush at 12 psi. The substrates used were two sizes of ITO coated glass slides (7 × 50 mm and 25 × 37.5 mm). Copper tape was adhered to the top of the slides to ensure an electrical connection.

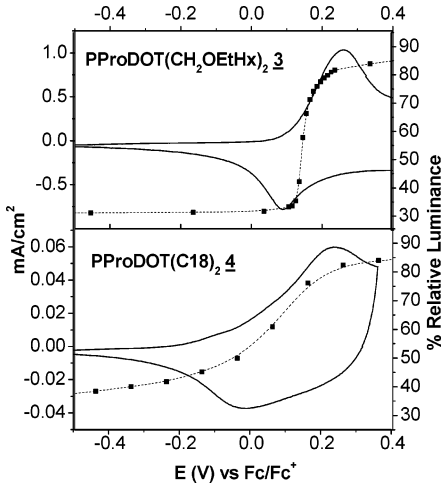

Figure 6. Percent relative luminance vs applied potential (dashed line) superimposed on cyclic voltammetry (solid line, 50 mV/s) for **PProDOT(CH$_2$OEtHx)$_2$** (**3**) (top) and **PProDOT(C18)$_2$** (**4**) (bottom).

was unable to be electrochemically polymerized/deposited onto a working electrode because of the difficulty in finding a suitable solvent that can dissolve the monomer, but will not dissolve the resulting polymer. **ProDOT(C18)$_2$** (**5**) is not soluble in acetonitrile, propylene carbonate, or solvent systems combining these solvents with toluene or methylene chloride. Chlorinated solvents, such as chloroform and methylene chloride, which do dissolve the monomer, also dissolved the oligomers/polymers as they formed, leading to films of poor quality which peel from the electrode after a few scans.

A second method of forming thin films by spray casting polymer solution (5 mg/mL in toluene) onto the desired substrate using an air brush (Testor Corps.) at 12 psi has been developed. Highly homogeneous films with thicknesses controlled from 30 to 500 nm, and surface roughnesses of 20 nm as determined by profilometry, were attained. A photograph of spray cast films of **PProDOT(CH$_2$OEtHx)$_2$** (**3**) (left) and **PProDOT(C18)$_2$** (**4**) (right) on ITO coated glass slides is shown in Figure 5.

All polymer films were electroactive and could be reversibly oxidized by cyclic voltammetry (CV). Table 3 lists the half-wave potentials for all spray cast and electropolymerized films taken from CV scans. The spray cast films have consistently higher half-wave potentials (∼ 60−150 mVs) than the electropolymerized films, which may be attributed to the more thorough incorporation of the electolyte salt. The half-wave potentials for electrodeposited films were similar to other alkylenedioxythiophene polymers with values close to −0.15 V. The $E_{1/2}$ increased 100−200 mV with an increase in the bulk of the substituents, which may indicate that they interfere in a minimal way with the conformation of the thiophene rings.

In comparing polymers with branched substituents to those with linear substituents, clear trends are observed in redox properties. The cyclic voltammograms (CVs) of **PProDOT(C18)$_2$** (**4**) and **PProDOT-(CH$_2$OEtHx)$_2$** (**3**) are seen in Figure 6. The luminance plot superimposed on the CVs will be discussed later in the section "Electrochromic Properties". **PProDOT-(CH$_2$OEtHx)$_2$** (**3**) has a slightly higher potential (0.0 V) at which the onset of oxidation occurs in comparison to **PProDOT(C18)$_2$** (**4**) (−0.3 V). Since the anodic peaks fall very close to one another, **PProDOT(CH$_2$OEtHx)$_2$** (**3**) shows a much sharper current response, while **PProDOT(C18)$_2$** (**4**) gives a more broad redox process. This trend is also observed in electrochemically polymerized and spray cast films of polymers **PProDOT(Hx)$_2$** (**1**) and **PProDOT(EtHx)$_2$** (**2**), suggesting that the late onset is an effect of the branching of the alkyl chain and not the formation of the film.

Optoelectronic Studies. Table 4 lists the major peaks in the UV−vis spectra of polymer solutions (1 mg/50 mL) and films as well as the optical band-gap taken for each film. The solution spectra were found to be slightly blue shifted from that of the films with less resolution of the fine structure. This is expected, due to the disorder of the polymer chains in solution, leading to a lower effective conjugation length.

The electrochemically polymerized films all exhibit a similar dark blue-purple color in the neutral state and are sky-blue transmissive when a sufficient potential is applied to fully oxidize the film. The color of the neutral state is similar to other electrochemically polymerized alkylenedioxythiophene polymers. The optical band-gaps ranged from 1.8 to 1.9 eV for all polymers except **PProDOT(EtHx)$_2$** (**2**), which fell at 1.96 eV. This small increase in band-gap is due to a sharper onset on the low energy end of the visible spectrum. The UV−vis spectra of the polymers often gave three peaks as

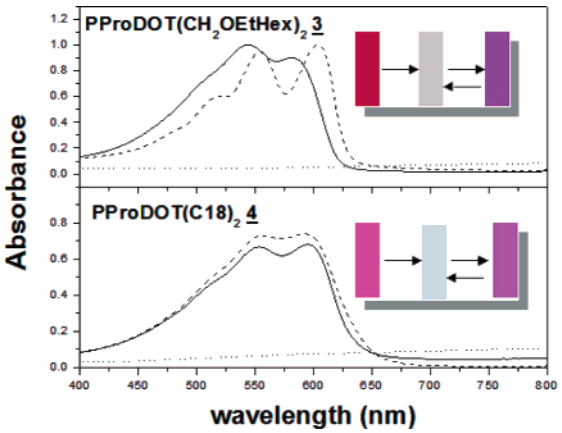

Figure 7. Optoelectronic spectra of spray cast films of PProDOT(CH_2OEtHx)$_2$ (**3**) (top) and PProDOT(C18)$_2$ (**4**) (bottom) which are neutral and unswitched (solid line), electrochemically oxidized (dotted line), and neutral after electrochemical switching (dashed line). The insets show the color swatches of spray cast films which are, from right to left, neutral and unswitched, electrochemically oxidized, and neutral after electrochemical switching.

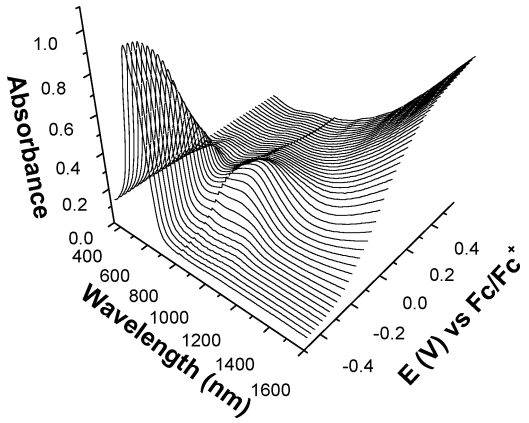

Figure 8. Three-dimensional surface of the spectroelectrochemistry of a previously switched spray cast film of **PProDOT(Hx)$_2$ (1)** on an ITO coated glass slide. Spectra were taken at 50 mV increments between −0.4 to 0.5 V vs Fc/Fc^+.

listed in Table 4, but each spectrum differed in intensity and resolution. These peaks have been attributed to vibronic coupling,[31] Davydov splitting,[32] or absorption of polymer segments with different, yet discrete, chain lengths.[11] The fine structure is much more resolved for the polymers **PProDOT(EtHx)$_2$** (**2**) and **PProDOT-(CH_2OEtHx)$_2$** (**3**), which have branched substituents. **PProDOT(Hx)$_2$** (**1**) and **PProDOT(Bu)$_2$** exhibit the peaks, but they exist as unresolved humps and the high energy peak exists only as a shoulder.

The as-made spray cast films, on the other hand, vary in the UV−vis peak values as well as the perceivable color of the films. Figure 5 shows a photograph of spray cast films of **PProDOT(CH_2OEtHx)$_2$** (**3**) (left, red color) and **PProDOT(C18)$_2$** (**4**) (right, deep purple color) on different sized ITO coated glass slides. Figure 7 shows the spectra of the as-made spray cast films, electrochemically oxidized spray cast films, and electrochemically switched neutral films along with the corresponding color swatches derived from colorimetry results for polymers **PProDOT(CH_2OEtHx)$_2$** (**3**) and **PProDOT-(C18)$_2$** (**4**).[36] Upon oxidation, the color of the films change from the highly absorbing state to a transmissive sky blue state comparable to the rest of the dioxythiophene family as the absorption in the 400−800 nm region is reduced in intensity. Upon reduction of these oxidatively doped films, the color switches to an absorptive dark blue-purple. The perceivable color of spray cast films of **PProDOT(C18)$_2$** (**4**) show a small change upon redox switching, while **PProDOT-(CH_2OEtHx)$_2$** (**3**) shows a more significant change from red to dark blue-purple, corresponding to a 20 nm red shift in the optical spectrum. This shift is attributed to a doping induced extension of the polymer chains giving a longer effective conjugation length, a phenomenom observed with **PProDOT(Bu)$_2$**.[25] The quinoid geometry of the oxidized state leads to an ordering of the chains.[33] After reduction, the extension of the chains is partially preserved, leading to a larger effective conjugation length compared to the as-made spray cast films. **PProDOT(Hx)$_2$** (**1**) exhibited behavior similar to that of **PProDOT(CH_2OEtHx)$_2$** (**3**), switching from red to transparent when oxidized and then to dark blue-purple upon electrochemical reduction. The spray cast film of **PProDOT(EtHx)$_2$** (**2**) is purple, a slight difference as perceived by the human eye in comparison to that of the electrochemically polymerized film. The lack of doping induced chain extension and the purple color of the as-made spray cast films of **PProDOT(EtHx)$_2$** (**2**) and **PProDOT(C18)$_2$** (**4**) is surprising and is an indication of how a small change in the structure can lead to different optical properties in the solid state. The original colors were inaccessible after the first redox process. The optical band-gaps of the spray cast films after switching were similar to the electrodeposited films, ranging from 1.8 to 2.0 eV.

A full spectroelectrochemical series was performed on electrodeposited and spray cast films of all polymers in 50 mV increments as illustrated for a spray cast film of **PProDOT(Hx)$_2$** (**1**) (see Figure 8). As the working potential increases, the absorbance in the visible region decreases, as transitions at ∼950 and ∼1600 nm start to grow. At higher potentials, the $\pi-\pi^*$ transition continues to decrease as the 950 nm peak levels out and the 1600 nm peak continues to grow. These NIR peaks are attributed to charge carriers that form due to oxidation of the film. By removal of one electron, a polaron structure is formed, giving rise to the 950 and 1600 peaks.[34,35] At high potentials, a second electron will be lost, forming a bipolaron structure which is associated with a second overlapping peak also at ∼1600 nm. The overall effect of oxidizing the film is a bleaching of the dark blue-purple color to a more transmissive sky blue. The three-dimensional plot of the spray cast film of **PProDOT(Hx)$_2$** (**1**) is representative of all alkylenedioxythiophene polymers.

Figure 9 compares the spectroelectrochemistry of spray cast films of **PProDOT(CH_2OEtHx)$_2$** (**3**) and **PProDOT(C18)$_2$** (**4**) in transmittance mode in order to probe the potential dependence of the colored to transmissive transition. We find that for **PProDOT(C18)$_2$** (**4**) (top), the change in transmittance in the visible region occurs gradually over a 600 mV region. The spectral series for **PProDOT(CH_2OEtHx)$_2$** (**3**) (bottom), on the other hand, exhibit a distinctly sharper change in transmittance as a function of voltage. More than 60% of the total transmittance change in the visible region occurs in a 120 mV potential range (between 0.13 and 0.25 V vs Fc/Fc^+). This sharp change in the electronic properties with small potential changes is also observed for **PProDOT(EtHx)$_2$** (**2**), suggesting that this behavior is associated with the branched alkyl derivatives.

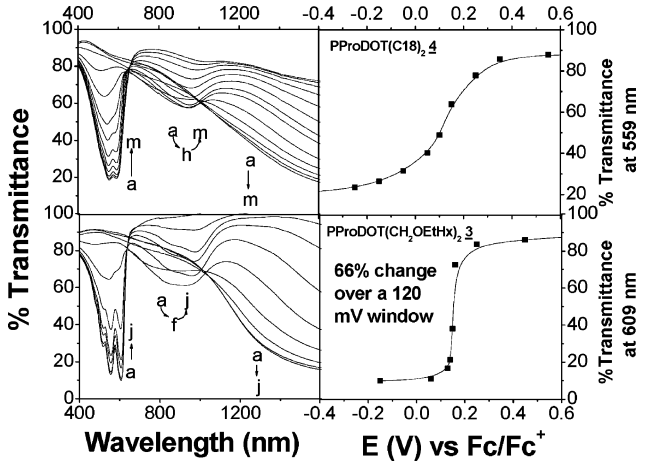

Figure 9. Top left: Spectroelectrochemistry of a previously switched spray cast polymer film of **PProDOT(C18)$_2$** (**4**) at applied potentials of (a) −0.95, (b) −0.65, (c) −0.45, (d) −0.25, (e) −0.15, (f) −0.05, (g) +0.05, (h) +0.11, (i) +0.15, (j) 0.25, (k) +0.35, (l), +0.55, and (m) +0.75 V vs Fc/Fc.$^+$ Top right: Percent transmittance as a function of applied potential taken at 559 nm from the spectroelectrohemistry of **PProDOT(C18)$_2$** (**4**). Bottom left: Spectroelectrochemistry of a previously switched spray cast film of **PProDOT(CH$_2$OEtHx)$_2$** (**3**) at applied potentials of (a) −0.15, (b) +0.06, (c) +0.13, (d) +0.14, (e) +0.15, (f) +0.16, (g) +0.25, (h) +0.45, (i) +0.65, and (j) +0.85 V vs Fc/Fc.$^+$ Bottom right: Percent transmittance as a function of applied potential taken at 609 nm from the spectroelectrochemistry of **PProDOT(CH$_2$OEtHx)$_2$** (**3**).

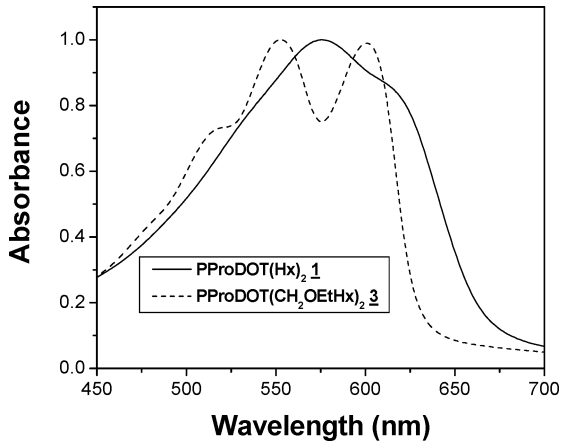

Figure 10. Visible spectra of spray cast films of **PProDOT-(Hx)$_2$** (**1**) (solid line) and **PProDOT(CH$_2$OEtHx)$_2$** (**3**) (dotted line). **PProDOT(CH$_2$OEtHx)$_2$** (**3**) shows less tailing on the low energy side in comparison to **PProDOT(Hx)$_2$** (**1**).

Although the fundamental reason for this structure−property trend is unknown at this time, it is postulated that the branched chains interact with the thiophene backbone to limit the effective conjugation length. This provides a more distinct onset for the absorption on the low energy end due to a decrease in the population of chains with long effective conjugation lengths. Figure 10 compares the visible spectra of spray cast polymer films of **PProDOT(Hx)$_2$** (**1**) and **PProDOT-(CH$_2$OEtHx)$_2$** (**3**). **PProDOT(Hx)$_2$** (**1**) has a lower band-gap due to the extension of the absorption into the low energy end while the absorbance of **PProDOT-(CH$_2$OEtHx)$_2$** (**3**) drops distinctly at wavelengths longer than 600 nm. If the chains all have a smaller range of effective conjugation lengths, this will lead to a more distinct threshold voltage and give the film a smaller potential window where the color transition occurs.

Table 5. Electrochromic Properties of Spray Cast Films

	% ΔY	% ΔT	t (s)
PProDOT(Bu)$_2$	51	51	0.23
1	58	70	0.37
2	70	79	0.73
3	56	80	0.57
4	42	51	2.2

Table 6. Electrochromic Properties of Electrochemically Deposited Films

	% ΔY	% ΔT	t (s)
PProDOT(Bu)$_2$	50	76	0.45
1	57	71	0.43
2	41	53	0.50
3	46	48	0.60

Electrochromic Properties. Recent studies on **PProDOT(Bu)$_2$** found that the electrochemically polymerized films gave a higher contrast ratio than drop cast films from toluene solution.[25] The drop cast films were inhomogeneous and tended to crack and peel upon switching with morphologies that tend to be compact with inconsistent thicknesses. The spray cast films used for the current studies, on the other hand, gave highly homogeneous films of consistent thicknesses and low surface roughness. Table 5 lists the change in relative luminance, singular wavelength percent transmittance contrast ratios, and 95% switching times for the spray cast films of 150−250 nm thickness while Table 6 lists the values for the electrochemically polymerized films deposited in the same thickness range. By comparing the values obtained in Tables 5 and 6, it is readily seen that the electrochromic properties of the spray cast films are now comparable to the electrodeposited films, which suggests these polymers will prove useful for large area electrochromic devices where processing is important.[26]

Relative luminance studies (% ΔY) between fully reduced and oxidized states were performed as a function of potential on all polymers using the CIE 1931 Yxy color space.[36] The luminance is a measure of the transmissivity of a material to visible light calibrated to the sensitivity of the human eye, making it a valuable technique for measuring electrochromic materials that change from colorful absorptive states to transmissive states. The % ΔY values for spray cast films range from 40 to 60% while the values for electrodeposited films range from 45 to 60%. These values compare to other known absorptive/transmissive electrochromic polymers such as PProDOT(Me)$_2$ (% ΔY = 61%) and exceed the unsubstituted parent, PEDOT (% ΔY = 33%).

By superimposing the CV and relative luminance results, the relationship between the electrochemical properties and the optical properties of the film are readily seen. Figure 6 shows the relative luminance trace with the current response for spray cast films of **PProDOT(CH$_2$OEtHx)$_2$** (**3**) (top) and **PProDOT-(C18)$_2$** (**4**) (bottom). **PProDOT(C18)$_2$** (**4**) (bottom) shows a gradual change, beginning at −1.0 V and continuing until saturation is reached at 0.25 V. **PProDOT(CH$_2$OEtHx)$_2$** (**3**), by comparison, gives a much sharper transition for both the CV and % Y results, undergoing zero luminance change until the potential reaches 0.1 V, consistent with spectroelectrochemical studies discussed earlier. Beyond this potential, the polymer exhibits a 44% change in relative luminance with a 100 mV potential increase. The linear chain polymers, **PProDOT(Hx)$_2$** (**1**) and **PProDOT-(Bu)$_2$**, show broad curves similar to **PProDOT(C18)$_2$**

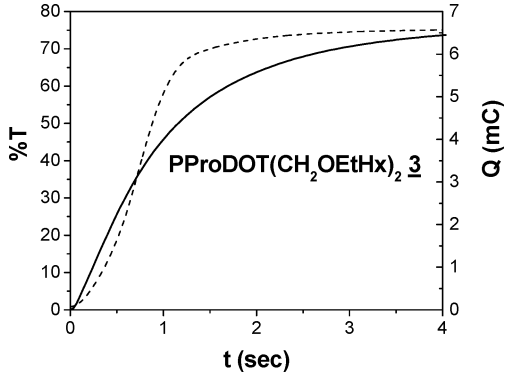

Figure 11. Percent transmittance vs time (dashed line) superimposed upon charge vs time (solid line) measured during a potential switch between −0.5 and +1.2 V vs Fc/Fc^+ on a spray cast polymer film of **PProDOT(CH$_2$OEtHx)$_2$ (3)**.

(**4**). **PProDOT(EtHx)$_2$** (**2**) shows a sharp transition in the luminance as a function of potential similar to **PProDOT(CH$_2$OEtHx)$_2$** (**3**), demonstrating the effects of linear vs branched derivatives on electrochromic properties.

Switching studies of spray cast and electrodeposited polymer films were performed by monitoring the % *T* at λ_{max} as a funtion of time during a potential step where the polymer oxidizes and reduces. The switching times, taken at 95% of the full switch, give subsecond times for all films with the exception of **PProDOT(C18)$_2$** (**4**). Earlier studies showed that increasing the number of substituents on the alkylenedioxy ring decreased the switching time substantially.[21] Increasing steric bulk of the substituents, on the other hand, does not significantly decrease the switching time as polymers **1**−**3** gave similar values. **PProDOT(C18)$_2$** (**4**) gave a much higher value at 2.2 s. The long alkyl chains likely decrease ion flux, leading to longer switching times.

Coloration Efficiency. Composite coloration efficiency is the change in optical density as a function of charge passed as given by eq 1

$$\eta = \Delta OD/Q_d \quad (1)$$

where ΔOD is the change in optical density and Q_d is the charge passed in order for the change to occur.

The optical density change is determined by measuring the % *T* at λ_{max} before and after a full switch using eq 2.

$$\Delta OD = \log(\%\ T_1/\%\ T_2) \quad (2)$$

Figure 11 shows the relationship between the charge and % *T* as a function of time for a spray cast film of **PProDOT(CH$_2$OEtHx)$_2$** (**3**). The composite coloration efficiency can be calculated at any time, but we have chosen to report a value at 95% of the full switch in order to allow direct comparison of different systems.[37] An earlier study obtained values of 375 cm^2/C for electrodeposited films of PProDOT(Me)$_2$ while PEDOT, in comparison, was found to have CE values of 186 cm^2/C. Although the charge needed for the switch to occur was similar for both polymers, PProDOT(Me)$_2$ gave twice the change in optical density as did PEDOT, leading to a CE value roughly twice as large.

Table 7 lists the composite coloration efficiency values for spray cast and electrodeposited films of all films taken at 95% of the full switch. The CE values obtained are two to three times larger than PProDOT(Me)$_2$ films

Table 7. Coloration Efficiency Values for Spray Cast and Electrodeposited Films

	CE(cast)[a] (cm^2/C)	CE(echem)[b] (cm^2/C)
PProDOT(Bu)$_2$	1137	1365
1	833	1270
2	1050	1204
3	1235	1232
4	472	NA

[a] Composite coloration efficiency taken at 95% of a full switch for electrochemically deposited films of 150 nm thickness. [b] Composite coloration efficiency taken at 95% of a full switch for previously switched spray cast films of 150 nm thickness.

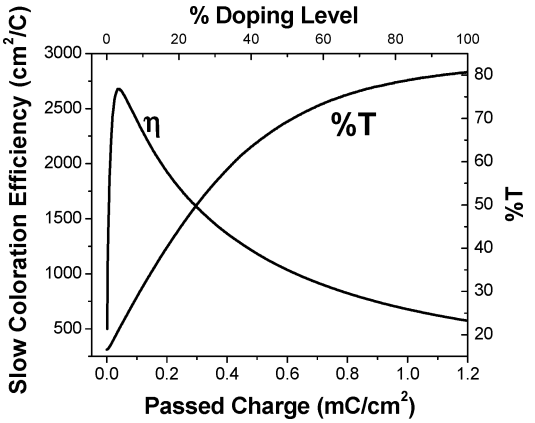

Figure 12. Slow coloration efficiency and percent transmittance vs passed charge for a 150 nm film of **PProDOT-(CH$_2$OEtHx)$_2$** (**3**).

with the exception of **PProDOT(C18)$_2$** (**4**). Since the change in optical density is similar to PProDOT(Me)$_2$ films, the increase in composite CE values is due to a decrease in charge needed to oxidize the films. One possible explanation is that the conductivity of the neutral state is higher for these polymers, leading to less current loss, which would increase the CE.

We have also measured the coloration efficiencies of all spray cast films by passing a low constant current leading to bleaching of the films over a period of 20 s. As an example, Figure 12 shows the change in the transmittance of a film of **PProDOT(CH$_2$OEtHx)$_2$** (**3**), along with the variation of the coloration efficiency, as a function of the amount of charge passed during this slow bleaching. The overall transmitance contrast (% $\Delta T = 65\%$) for the slow switching of this film is similar to those observed with the large potential step switching experiment. The η value undergoes a maximum at ∼2680 cm^2/C as this is the initial coloration efficiency and follows a form similar to that observed previously in the literature.[38] The other polymers had peak values ranging from 650 to 2350 cm^2/C. Considering the physical significance of the peak η values, this can be taken as the coloration efficiency for the initial change during the electrochromic switch. A peak is observed as the electrode charges (e.g., double layer) and the optical response lags the current slightly when Faradaic doping begins. Although the charging process is linear with time (constant current), the % *T* curve tends to saturate and this results in lower η values at higher doping levels.

Conclusions

Four new organic solvent soluble and spray processable disubstituted propylenedioxythiophene polymers have been synthesized by Grignard metathesis polym-

erization on the 1−5 g scale. The substituents used were designed to increase polymer solubility, while maintaining the desirable electrochromic properties of less soluble derivatives. A technique to spray cast polymer solutions onto ITO coated glass slides to form highly homogeneous thin films was developed, which greatly improved the electrochromic properties in comparison to earlier reported drop cast films, exhibiting a dark blue-purple color when neutral and a sky-blue transmissive color when oxidized. The relative luminance change ranged from 40 to 60%, a comparable value to the rest of the alkylenedioxythiophene family,[36] and subsecond switching times were found to be independent of structure or film formation with the exception of the long alkyl chain derivative, **PProDOT(C18)$_2$ (4)**. The CE values of all polymers exceeded the largest previously reported value for poly(alkylenedioxythiophenes).[37] The desirable electrochromic properties, ease in synthesis, solubility, film processability, and high coloration efficiency values make these materials excellent candidates for use in large area electrochromic devices. A distinct structure−property relationship was observed in this series of polymers. The polymers with branched substituents had higher band-gaps and the color change occurred over a smaller voltage range in comparison to the polymers with linear substituents. This is postulated to be due to a limited effective conjugation length allowed in the solid state when branched substituents are present. Further studies are underway to understand this relationship.

Experimental Section

Instrumentation. GPC was performed on two 300 × 7.5 mm Polymer Laboratories PLGel 5 μM mixed-C columns with Waters Associates liquid chromatography 757 UV absorbance detector at 585 nm or a 2996 photodiode array detector. Polymer solutions were prepared in THF and filtered through a 50 μM filter before injection. A constant flow rate of 1 mL/min was used. Molecular weights were obtained relative to polystyrene standards. MALDI−TOF mass spectrometry was performed with a Bruker ProFLEX III reflectron instrument with delayed extraction. HABA (2-(4-hydroxyphenylazo)benzoic acid) and terthiophene matrices were used. NMR spectra were recorded on a Gemini 300 FT-NMR or a VXR 300 FT-NMR. High-resolution mass spectrometry was carried out on a Finnigan MAT 95Q mass spectrometer. Electrochemical studies were carried out using an EG&G PAR model 273A potentiostat/galvanostat in a three electrode cell configuration consiting of a Ag° wire pseudo reference electrode calibrated with a Fc/Fc$^+$ couple, a glassy carbon button, platinum button, or ITO-coated glass slide (7 × 50 × 0.6 mm, 20 Ω/cm) as the working electrode, and a Pt flag as the counter electrode in a 0.1 M tetrabutylammonium hexafluorophospate propylene carbonate solution. All absorption spectra from thermochromism, spectroelectrochemistry, and switching studies were carried out on a Varian Cary 500 scan UV−vis−NIR spectrophotometer. Thermochromism was performed using a SPV 1 × 1 Varian Cary duel cell peltier accessory. Colorimetry was carried out using a Minolta CS-100 Chroma Meter and CIE recommended normal/normal (0/0) illuminating/viewing geometry for transmittance measurements.[36] The sample was illuminated from behind with a D50 (5000 K) light source in a light booth specially designed to exclude external light. Fluorescence data was collected with a Spex F-112 photon counting fluorimeter at room temperature. Emission quantum yields were measured relative to Rhodamine 6G and Coumarin 6 in methanol where $\phi_f = 1.00$, and optical density of solutions was kept below $A = 0.1$. The film fluorescence was carried out according to a known procedure.[39]

Synthesis. 3,4-Dimethoxythiophene was synthesized using a known procedure.[40] 2,2-bis(bromomethyl)-1,3-propanediol, hexyl bromide, 2-ethylhexyl bromide, diethyl malonate, octadecanol, 2-ethylhexanol, 1.0 M MeMgBr in butyl ether, and all other inorganic reagents and solvents were purchased from Aldrich. Toluene was distilled over sodium before use. THF was dispensed from a pure pack anhydrous keg and further dried by an aluminum oxide column.

General Procedure for the Synthesis of Alkylated Diethyl Malonate. In a 5 L flame dried three-neck round-bottom flask equipped with an argon inlet, a condenser, and an addition funnel were combined 2 L of dry THF, 3.5 mol of alkyl bromide (3 equiv), and 3.5 mol of NaH. The flask was cooled to 0 °C, and 1.15 mol of freshly distilled diethyl malonate was added dropwise through the addition funnel. When the addition of the malonate was completed, the mixture was refluxed overnight. The flask was then cooled at 0 °C and the remaining sodium hydride was quenched by adding water dropwise. The mixture was then poured into brine (2 L), extracted two times with ether, and washed with brine. The solvent and the alkyl bromide were removed under vacuum. The crude oil obtained was then used in the next step without further purification.

General Procedure for the Synthesis of Diols 9 and 10. In a 5 L flame dried three-neck round-bottom flask equipped with an argon inlet, a condenser, and an addition funnel were combined 2 L of dry ethyl ether and 1.7 mol of $LiAlH_4$ powder. The crude dialkyl malonate (1.13 mol) was added dropwise at 0 °C. When the addition was completed, the mixture was allowed to warm to room temperature. The reaction mixture was stirred under argon for 20 h.

2,2-Dihexylpropane-1,3-diol (9). ^{1}H NMR (300 MHz, $CDCl_3$): δ 3.59 (d, 4H, J = 5.3 Hz), 2.39 (t, 2H, J = 5.3 Hz), 1.40−1.10 (m, 20H), 0.90 (t, 6H, J = 7.3 Hz). ^{13}C NMR (75 MHz, $CDCl_3$): δ 69.7, 41.2, 32.0, 31.1, 30,5, 29.9, 23.1, 22.9, 14.3. HRMS: calcd for $C_{15}H_{32}O_2$, 245.2481; found, 245.2475. Anal. Calcd for $C_{15}H_{32}O_2$: C, 73.71; H, 14.20. Found: C, 74.12; H, 14.18.

2,2-Bis(2-ethylhexyl)-propane-1,3-diol (10). ^{1}H NMR (300 MHz, $CDCl_3$): δ 3.65 (s, 4H), 2.41 (s, 2H), 1.40−1.10 (m, 22H), 0.95−0.80 (m, 12H). ^{13}C NMR (75 MHz, $CDCl_3$): δ 70.1, 42.8, 37.1, 34.9, 33.7, 29.0, 27.9, 23.4, 14.4, 10.8. HRMS: calcd for $C_{19}H_{41}O_2$ $(M + H)^+$, 301.3106; found, 301.3103. Anal. Calcd for $C_{19}H_{40}O_2$: C, 75.94; H, 13.42. Found: C, 75.95; H, 12.35.

General Procedure for the Transetherification of 3,4-Dimethoxythiophene with Diols. First, 21 mmol of 3,4-dimethoxythiophene, 42 mmol of diol, 2.1 mmol of *p*-toluenesulfonic acid, and 200 mL of toluene were combined in a 500 mL flask equipped with a Soxhlet extractor with type 4A molecular sieves in a cellulose thimble. The solution was refluxed overnight. The reaction mixture was cooled and washed once with water. The toluene was removed under vacuum, and the crude product was purified by column chromatography on silica gel with 3:2 hexanes/methylene chloride.

3,3-Bis(bromomethyl)-3,4-dihydro-2*H*-thieno[3,4-*b*][1,4]-dioxepine [ProDOT(CH_2Br)$_2$]. Yield: 5.2 g of white crystalline solid (73%). Mp: 66−68 °C. ^{1}H NMR (300 MHz, $CDCl_3$): δ 6.49 (s, 2H), 4.10 (s, 4H), 3.61 (s, 4H). ^{13}C NMR (75 MHz, $CDCl_3$): δ 148.5, 105.7, 74.1, 46.1, 34.4. HRMS calcd for $C_9H_{10}O_2Br_2S$, 339.8768; found, 339.8820. Anal. Calcd for $C_9H_{10}O_2Br_2S$: C, 31.60; H, 2.95; S, 9.37 Found: C, 31.83; H, 2.99; S, 9.20.

3,3-Dihexyl-3,4-dihydro-2*H*-thieno[3,4-*b*][1,4]dioxepine [ProDOT(Hx)$_2$, 11]. Yield: 10.7 g of clear oil (95%). ^{1}H NMR (300 MHz, $CDCl_3$): δ 6.42 (s, 2H), 3.88 (s, 4H), 1.45−1.20 (m, 20 H), 0.95−0.82 (m, 6H). ^{13}C NMR (75 MHz, $CDCl_3$): δ 149.9, 104.9, 77.8, 43.9, 32.0, 32.0, 30.4, 23.0, 22.9, 14.3. HRMS: calcd for $C_{19}H_{32}O_2S$, 324.2123; found, 324.2120. Anal. Calcd for $C_{19}H_{32}O_2S$: C, 70.32; H, 9.94; S, 9.88 Found: C, 70.48; H, 10.48; S, 9.78.

3,3-Bis(2-ethylhexyl)-3,4-dihydro-2*H*-thieno[3,4-*b*][1,4]-dioxepine [ProDOT(EtHx)$_2$, 12] The crude oil obtained was purified by column chromatography (3:2) hexanes/dichloromethane followed by another column using 3:1 hexanes/dichloromethane to afford 6.0 g of clear oil (57%). ^{1}H NMR (300 MHz, $CDCl_3$): δ 6.43 (s, 2H), 3.93 (s, 4H), 1.2−1.5 (m,

22H), 0.75−1.0 (m, 12H). ^{13}C NMR (300 MHz, $CDCl_3$): δ 150.0, 104.61, 78.0 (t), 45.5, 38.7, 35.0, 33.8, 29.0, 28.0, 23.3, 14.4, 10.8. HRMS: calcd for $C_{23}H_{40}O_2S$, 380.2749; found, 380.2753. Anal. Calcd for $C_{23}H_{40}O_2S$: C, 72.58; H, 10.59; S, 8.42. Found: C, 72.78; H, 10.30; S, 8.24.

General Procedure for the Williamson Etherification of ProDOT(CH_2Br)$_2$. A 250 mL flame dried round-bottom flask filled with 50 mL of DMF, 8.7 mmol of alcohol (3 equiv), and 17.5 mmol of NaH (6 equiv) was heated at 110 °C overnight. Then 2.9 mmol of **ProDOT(CH_2Br)$_2$** was added and the reaction continued at 110 °C for another 24 h. After completion, the flask was cooled and added to 200 mL of brine and extracted three times with ethyl ether. The organic layer was then washed three times with water and dried over magnesium sulfate, and the solvent was removed by rotary evaporation under reduced pressure. The resulting crude product was purified by column chromatography.

3,3-Bis(octadecyloxymethyl)-3,4-dihydro-2*H*-thieno-[3,4-*b*][1,4]dioxepine [ProDOT(C18)$_2$, 5]. The orange solid obtained was purified by column chromatography (3:2 hexanes, methylene chloride) to afford 0.86 g of white solid (68%). Mp: 48−50 °C. ^{1}H NMR (300 MHz, $CDCl_3$): δ 6.44 (s, 2H), 4.00 (s, 4H), 3.48 (s, 4H), 3.39 (t, 4H, J = 6.6 Hz), 1.53 (m, 4H), 1.25 (m, 64H), 0.88 (t, 6H, J = 6.9 Hz). ^{13}C NMR (75 MHz, $CDCl_3$): δ 149.9, 105.2, 73.9, 71.9, 69.7, 47.9, 32.1, 29.75, 26.3, 22.9, 14.3. HRMS: calcd for $C_{45}H_{84}O_4S$, 720.6090; found, 720.6047. Anal. Calcd for $C_{45}H_{84}O_4S$: C, 74.94; H, 11.74; O, 8.87; S, 4.45. Found: C, 74.69; H, 11.37; O, 9.19; S, 4.33.

3,3-Bis(2-ethylhexyloxymethyl)-3,4-dihydro-2*H*-thieno-[3,4-*b*][1,4]dioxepine [ProDOT($CH_2OEtHex$)$_2$, 6]. The crude oil obtained was purified by column chromatography (CH_2Cl_2) to afford 1.8 g of clear oil (70%). ^{1}H NMR (300 MHz, $CDCl_3$): δ 6.42 (s,4H), 3.98 (s, 4H), 3.44 (s, 4H), 3.25 (d, 4H), 1.2−1.6 (m, 18H), 0.8−1.0 (m, 12H). ^{13}C NMR (75 MHz, $CDCl_3$): δ, 149.7, 104.9, 74.3, 73.8, 69.8, 47.9, 39.6, 30.7, 29.1, 24.0, 23.1, 14.1, 11.1. HRMS: calcd for $C_{25}H_{44}O_4S$, 440.2960; found, 440.2964. Anal. Calcd for $C_{25}H_{44}O_4S$: C, 68.14; H, 10.06; S, 7.28. Found: C, 68.17; H, 10.39; S, 7.26.

General Procedure for the Bromination of ProDOT Derivatives. In a two-neck 250 mL round-bottom flask filled with 80 mL of chloroform, 1.5 g (2.1 mmol) of ProDOT was added and the solution was bubbled under argon for 20 min. Then 1.12 g (6.3 mmol) *N*-bromosuccinimde was added, and the solution was stirred for 20 h. After completion, the solvent was removed by rotary evaporation under reduced pressure, and the resulting residue was purified by column chromatography (4:1 hexanes/methylene chloride).

6,8-Dibromo-3,3-bis(octadecyloxymethyl)-3,4-dihydro-2*H*-thieno[3,4-*b*][1,4]dioxepine [ProDOT(C18)$_2$Br$_2$, 7]. The white solid obtained was purified by column chromatography (4:1 hexanes, methylene chloride) and recrystallized from CH_2Cl_2 to afford 1.64 g (90%) of white crystals. Mp: 65−66 °C ^{1}H NMR (300 MHz, $CDCl_3$): δ 4.07 (s, 4H), 3.46 (s, 4H), 3.38 (t, 4H, J = 6.6 Hz), 1.50 (m, 4H), 1.25 (m, 64H), 0.87 (t, 6H, J = 6.9). ^{13}C NMR (75 MHz, benzene-d_6) 148.1, 91.8, 72.1, 69.7, 48.3, 32.7, 30.6, 30.2, 26.9, 23.5, 14.7. HRMS: calcd for $C_{45}H_{82}O_4SBr_2$: 876.4301 Found: 876.4305. Anal. Calcd for $C_{45}H_{82}O_4SBr_2$: C, 61.49; H, 9.40; O, 7.28; S, 3.65. Found: C, 61.36; H, 9.51; O, 7.45; S, 3.57.

6,8-Dibromo-3,3-bis(2-ethylhexyloxymethyl)-3,4-dihydro-2*H*-thieno[3,4-*b*][1,4]dioxepine [ProDOT($CH_2OEtHex$)$_2$-Br$_2$), 8]. Yield: 5.43 g of clear oil (98%). ^{1}H NMR (300 MHz, $CDCl_3$): δ 4.09 (s, 4H), 3.49 (s, 4H), 3.28 (d, 4H), 1.2−1.6 (m, 18H), 0.8−1.0 (m, 12H). ^{13}C NMR (300 MHz, $CDCl_3$): δ147.2, 91.0, 74.6, 70.0, 48.2, 39.9, 30.9, 29.4, 24.2, 23.3, 14.4, 11.4. HRMS: calcd for $C_{25}H_{42}O_4SBr_2$, 596.1171; found, 596.1161. Anal. Calcd for $C_{25}H_{42}O_4SBr_2$: C, 50.17; H, 7.07; S, 5.36. Found: C, 50.43; H, 7.09; S, 5.16.

6,8-Dibromo-3,3-dihexyl-3,4-dihydro-2*H*-thieno[3,4-*b*]-[1,4]dioxepine [ProDOT(Hx)$_2$Br$_2$, 13]. Yield: 14.4 g of clear oil (91%).^{1}H NMR (300 MHz, $CDCl_3$): δ 3.93 (s, 4H), 1.45−1.15 (m, 20H), 0.90 (t, 6H, J = 7.0 Hz); ^{1}H NMR (300 MHz, $CDCl_3$): δ 147.4, 104.8, 90.8, 78.3, 44.2, 31.9, 30.3, 22.9, 14.3. HRMS: calcd for $C_{19}H_{30}O_2SBr_2$, 480.0333; found, 480.0334. Anal. Calcd for $C_{19}H_{30}O_2SBr_2$: C, 47.31; H, 6.27; S, 6.65; Br, 33.13. Found: C, 47.83; H, 6.79; S, 6.88; Br, 32.79.

6,8-Dibromo-3,3-bis(2-ethylhexyl)-3,4-dihydro-2*H*-thieno[3,4-*b*][1,4]dioxepine [ProDOT(EtHx)$_2$Br$_2$, 14]. Yield: 6.3 g of clear oil (80%). ^{1}H NMR (300 MHz, $CDCl_3$): δ 4.00 (s, 4H), 1.15−1.5 (m, 22H), 0.8−1.0 (m, 12H). ^{13}C NMR (300 MHz, $CDCl_3$): δ 147.3, 90.5, 78.6, 45.8, 38.8, 35.0, 29.0, 28.0, 23.3, 14.4, 10.8. HRMS: calcd for $C_{23}H_{38}O_2SBr_2$, 538.0940; found, 538.0944. Anal. Calcd for $C_{23}H_{38}O_2SBr_2$: C, 51.31; H, 7.11; S, 5.96 Found: C, 51.28; H, 7.00; S, 6.04.

General Procedure for Grignard Metathesis Polymerization of ProDOT(R)$_2$Br$_2$. Into a flame dried 250 mL round-bottom flask were added dry THF (150 mL) and 3.4 mmol of ProDOT(R)$_2$Br$_2$ under argon. Then methylmagnesium bromide (3.75 mL, 3.45 mmol, 0.918 M) was slowly added by addition funnel. The mixture was then refluxed for 1 h. Afterward, the flask was cooled and Ni(dppp)Cl_2 (18.4 mg, 0.0341 mmol) was added and the reaction was heated at reflux overnight under argon. The solution was then cooled and the polymer was precipitated by pouring the solution in 400 mL of methanol. The dark purple solid was purified by Soxhlet extraction with methanol for 24 h, hexanes for 48 h, and finally chloroform for 24 h. The chloroform was evaporated under reduced pressure to afford purple solid.

Poly(3,3-bis-octadecyloxymethyl-3,4-dihydro-2*H*-thieno-[3,4-*b*][1,4]dioxepine [PProDOT(C18)$_2$, 4]. Yield: 1.27 g of purple solid (52%).^{1}H NMR (300 MHz, benzene-d_6): δ 4.30 (bs, 4H), 3.58 (bs, 4H), 3.35 (bs, 4H), 1.67 (bs, 4H), 1.40 (m, 64H), 0.96 (m, 6H). ^{13}C (75 MHz, benzene-d_6): δ 145.8, 115.0, 71.9, 48.3, 32.4, 30.4, 30.3, 30.2, 29.9, 26.8, 23.3, 14.5. GPC analysis: M_n = 33445 g mol^{-1}; M_w = 47958 g mol^{-1}; PDI = 1.43.

Poly(6,8-Dibromo-3,3-bis(2-ethyl-hexyloxymethyl)-3,4-dihydro-2*H*-thieno[3,4-*b*][1,4]dioxepine) [PProDOT(CH_2O-EtHx)$_2$, 3]. Yield: 0.350 g of purple solid (93%). ^{1}H NMR (300 MHz, benzene-d_6): δ 4.25 (bs, 4H), 3.58 (bs, 4H), 3.25 (bs, 4H), 1.62−1.30 (m, 22H), 1.09−0.99 (m, 12H). ^{13}C (75 MHz, benzene-d_6): δ 146.2, 115.3, 75.1, 74.8, 71.0, 48.7, 40.4, 31.6, 30.0, 25.0, 24.0, 14.9, 11.9. GPC analysis: M_n = 47300 g mol^{-1}; M_w = 74850 g mol^{-1}; PDI = 1.58.

Poly(3,3-bis(2-ethylhexyl)-3,4-dihydro-2*H*-thieno[3,4-*b*][1,4]dioxepine) [PProDOT(EtHx)$_2$, 2]. Yield: 1.05 g of purple solid (63%) ^{1}H NMR (300 MHz, $CDCl_3$): δ 4.19 (bs, 4H), 1.8−1.15 (m, 22H), 1.1−0.80 (m, 12H). ^{13}C (75 MHz, benzene-d_6): δ 146.0, 115.1, 78.9, 46.1, 38.7, 35.8, 34.4, 29.5, 24.1, 14.9, 11.5. GPC analysis: M_n = 42927 g mol^{-1}; M_w = 62602 g mol^{-1}; PDI = 1.46.

Poly(3,3-Dihexyl-3,4-dihydro-2*H*-thieno[3,4-*b*][1,4]dioxepine) [PProDOT(Hx)$_2$, 1]. Yield: 5.2 g of purple solid (62%).^{1}H NMR (300 MHz, $CDCl_3$): δ 3.95 (bs, 4H), 1.62−1.2 (m, 20H), 0.97−0.80 (m, 6H);^{13}C (75 MHz, benzene-d_6): δ 146.4, 115.3, 78.0, 44.3, 32.6, 31.0, 23.5, 14.8. GPC analysis: M_n= 38087 g mol^{-1}; M_w = 65893 g mol^{-1}; PDI = 1.73.

Acknowledgment. We gratefully acknowledge financial support from the AFOSR (F49620-03-1-0091) and the ARO MURI program (DAAD 19-99-1-0316). We acknowledge Garry B. Cunningham for his technical assistance with the solution and film fluorescence studies.

References and Notes

(1) *Handbook of Conducting Polymers*, 2nd ed.; Skotheim, T. A., Elsenbaumer, R. L., Reynolds, J. R., Eds.; Marcel Dekker: New York, 1998.

(2) Reddinger, J. L.; Reynolds, J. R. *Adv. Polym. Sci.* **1999**, *145*, 57.

(3) (a) Roncali, J. *Chem. Rev.* **1997**, *97*, 173. (b) Roncali, J. *Chem. Rev.* **1992**, *92*, 711.

(4) Granstrom, M.; Harrison, M. G.; Friend, R. H. In *Electrooptical Polythiophene Devices. Handbook of Oligo- and Polythiophenes*; Fichou, D., Ed.; Wiley-VCH Verlag GmbH: Weinheim, Germany, 1999; pp 405−458.

(5) McQuade, D. T.; Pullen, A. E.; Swager, T. M. *Chem. Rev.* **2000**, *100*, 2537.
(6) Novak, P.; Muller, K.; Santhanam, K. S. V.; Haas, O. *Chem. Rev.* **1997**, *97*, 207.
(7) Dimitrakopoulus, C. D.; Mascaro, D. J. *IBM J. Res. Dev.* **2001**, *45*, 11.
(8) (a) Rosseinsky, D. R.; Mortimer, R. J. *Adv. Mater.* **2001**, *13*, 783. (b) Monk, P. M. S.; Mortimer, R. J.; Rosseinsky, D. R. *Electrochromism: Fundamentals and Applications*; Wiley-VCH: Weinheim, Germany, 1995.
(9) Sato, M.; Tanaka, S.; Kaeriyama, K. *J. Chem. Soc., Chem. Commun.* **1986**, 873.
(10) Jen, K. Y.; Miller, G. G.; Elsenbaumer, R. L. *J. Chem. Soc., Chem. Commun.* **1986**, 1346.
(11) McCullough, R. D.; Ewbank, P. C. In *Handbook of Conducting Polymers*, 2nd ed.; Skotheim, T. A., Elsenbaumer, R. L., Reynolds, J. R., Eds.; Marcel Dekker: New York, 1998; p 225.
(12) (a) McCullough, R. D.; Lowe, R. D. *J. Chem. Soc., Chem. Commun.* **1992**, 70. (b) McCullough, R. D.; Lowe, R. D.; Jayarama, M.; Anderson, D. L. *J. Org. Chem.* **1993**, *58*, 904.
(13) (a) Chen, T.-A.; Rieke, R. D. *J. Am. Chem. Soc.* **1992**, *114*, 10087. (b) Iraqi, A.; Barker, G. W. *J. Mater Chem.* **1998**, *8*, 25. (c) Guillerez, S.; Bidan, G. *Synth. Met.* **1998**, *93*, 123.
(14) Loewe, R. S.; Khersonsky, S. M.; McCullough, R. D. *Adv. Mater.* **1999**, *11*, 250.
(15) Loewe, R. S.; Ewbank, P. C.; Liu, J.; Zhai, L.; McCullough, R. D. *Macromolecules* **2001**, *34*, 4324.
(16) Alkan, S.; Cutler, C.; Reynolds, J. R. *Adv. Funct. Mater.* **2003**, *13*, 331.
(17) Dietrich, M.; Heinze, J.; Heywang, G.; Jonas, F. *J. Electroanal. Chem.* **1994**, *369*, 87.
(18) Groenendaal, L.; Jonas, F.; Freitag, D.; Pielartzik, H.; Reynolds, J. R. *Adv. Mater.* **2000**, *12*, 481.
(19) Sankaran, B.; Reynolds, J. R. *Macromolecules* **1997**, *30*, 2582.
(20) Kumar, A.; Welsh, D. M.; Morvant, M. C.; Piroux, F.; Abboud, K. A.; Reynolds, J. R. *Chem. Mater.* **1998**, *10*, 896.
(21) Welsh, D. M.; Kumar, A.; Meijer, E. W.; Reynolds, J. R. *Adv. Mater.* **1999**, *11*, 1379.
(22) Reeves, B. D.; Thompson, B. C.; Abboud, K. A.; Smart, B. E.; Reynolds, J. R. *Adv. Mater.* **2002**, *14*, 717.
(23) Zong, K.; Madrigal, L.; Groenendaal, L.; Reynolds, J. R. *Chem. Commun.* **2002**, 2498.
(24) Groenendaal, L.; Zotti, G.; Aubert, P.-H, Waybright, S. M.; Reynolds, J. R. *Adv. Mater.* **2003**, *15*, 855.
(25) Welsh, D. M.; Kloeppner, L. J.; Madrigal, L.; Pinto, M. R.; Thompson, B. C.; Schanze, K. S.; Abboud, K. A.; Powell, D.; Reynolds, J. R. *Macromolecules*, **2002**, *35*, 6517.
(26) Cirpan, A.; Argun, A. A.; Grenier, C. R. G.; Reeves, B. D.; Reynolds, J. R. *J. Mater. Chem.* **2003**, *13*, 2422.
(27) Joshi, V. S.; Bhide, B. V. *J. Indian Chem. Soc.* **1960**, *37*, 461.
(28) Liu, J.; Loewe, R. S.; McCullough, R. D. *Macromolecules* **1999**, *32*, 5777.
(29) *Electronic Materials: The Oligomer Approach;* Mullen, K., Wegner, G., Eds.; Wiley-VCH: Weinheim, Germany, 1998.
(30) (a) Leclerc, M. *Adv. Mater.* **1999**, *11*, 1491. (b) Garreau, S.; Leclerc, M.; Errien, N.; Louran, G. *Macromolecules* **2003**, *36*, 692.
(31) Sakurai, K.; Tachibana, H.; Shiga, N.; Terakura, C.; Matsumoto, M.; Tokura, Y. *Phys. Rev. B* **1997**, *56*, 9552.
(32) Politis, J. K.; Nemes, J. C.; Curtis, M. D. *J. Am. Chem. Soc.* **2001**, *123*, 2537.
(33) Apperloo, J. J.; Janssen, R. A.; Nielsen, M. M.; Bechgaard, K. *Adv. Mater.* **2000**, *12*, 1594.
(34) (a) Bredas, J. L.; Street, G. B. *Acc. Chem. Res.* **1985**, *18*, 309. (b) Bredas, J. L.; Scott, J. C.; Yakushi, K.; Street, G. B. *Phys. Rev.* **1984**, *30*, 1023.
(35) Aperloo, J. J.; van Haare, J. A. E.; Janssen, J. *Synth. Met.* **1999**, *101*, 417.
(36) Thompson, B. C.; Schottland, P.; Zong, K.; Reynolds, J. R. *Chem. Mater.* **2000**, *12*, 1563.
(37) Gaupp, C. L.; Welsh, D. M.; Rauh, R. D.; Reynolds, J. R. *Chem. Mater.* **2002**, *14*, 3964.
(38) Rauh, R. D.; Wang, F.; Reynolds, J. R.; Meeker, D. L. *Electrochim. Acta* **2001**, *46*, 2023.
(39) Pålsson, L.; Monkman, A. P. *Adv. Mater.* **2002**, *14*, 757.
(40) (a) Goldoni, F.; Langeveld-Voss, B. M. W.; Meijer, E. W. *Synth. Commun.* **1998**, *28*, 223. (b) Langeveld-Voss, B. M. W.;. Janssen, R. A. J.; Christiaans, M. P. T.;. Meskers, S. C. J.; Dekkers, H. P. J. M.; Meijer, E. W. *J. Am. Chem. Soc.* **1996**, *118*, 4908.

MA049222Y